


Mice with *GNAO1* R209H Movement Disorder Variant Display Hyperlocomotion Alleviated by Risperidone^S

Cassandra L. Larrivee, Huijie Feng, Josiah A. Quinn, Vincent S. Shaw, Jeffrey R. Leipprandt, Elena Y. Demireva, Huirong Xie, and  Richard R. Neubig

Department of Comparative Medicine and Integrative Biology (C.L.L.), Department of Pharmacology and Toxicology (C.L.L., H.F., J.A.Q., V.S.S., J.R.L., R.R.N.), Transgenic and Genome Editing Facility, Institute for Quantitative Health Science and Engineering (E.Y.D., H.X.), and Nicholas V. Perricone, M.D., Division of Dermatology, Department of Medicine (R.R.N.), Michigan State University, East Lansing, Michigan

Received September 28, 2019; accepted December 27, 2019

ABSTRACT

Neurodevelopmental disorder with involuntary movements (Online Mendelian Inheritance in Man: 617493) is a severe, early onset neurologic condition characterized by a delay in psychomotor development, hypotonia, and hyperkinetic involuntary movements. Heterozygous de novo mutations in the *GNAO1* gene cause neurodevelopmental disorder with involuntary movements. $G\alpha_o$, the gene product of *GNAO1*, is the alpha subunit of G_o , a member of the heterotrimeric $G_{i/o}$ family of G proteins. G_o is found abundantly throughout the brain, but the pathophysiological mechanisms linking $G\alpha_o$ functions to clinical manifestations of *GNAO1*-related disorders are still poorly understood. One of the most common mutant alleles among the *GNAO1* encephalopathies is the c.626G>A or p.Arg209His (R209H) mutation. We developed heterozygous knock-in *Gnao1*^{+/R209H} mutant mice using CRISPR/Cas9 methodology to assess whether a mouse model could replicate aspects of the neurodevelopmental disorder with involuntary movements clinical pattern. Mice carrying the R209H mutation exhibited increased locomotor activity and a modest gait abnormality at 8–12 weeks. In contrast to mice carrying other mutations in *Gnao1*, the *Gnao1*^{+/R209H} mice did not show

enhanced seizure susceptibility. Levels of protein expression in multiple brain regions were unchanged from wild-type (WT) mice, but the nucleotide exchange rate of mutant R209H $G\alpha_o$ was 6.2× faster than WT. The atypical neuroleptic risperidone has shown efficacy in a patient with the R209H mutation. It also alleviated the hyperlocomotion phenotype observed in our mouse model but suppressed locomotion in WT mice as well. In this study, we show that *Gnao1*^{+/R209H} mice mirror elements of the patient phenotype and respond to an approved pharmacological agent.

SIGNIFICANCE STATEMENT

Children with de novo mutations in the *GNAO1* gene may present with movement disorders with limited effective therapeutic options. The most common mutant variant seen in children with *GNAO1*-associated movement disorder is R209H. Here we show, using a novel *Gnao1*^{+/R209H} mouse, that there is a clear behavioral phenotype that is suppressed by risperidone. However, risperidone also affects wild-type mouse activity, so its effects are not selective for the *GNAO1*-associated movement disorder.

Introduction

$G\alpha_o$ is the alpha subunit of the heterotrimeric G protein G_o . It is the most abundant heterotrimeric G protein in the central nervous system, comprising 1% of mammalian brain membrane protein. Mutations in *GNAO1*, which encodes $G\alpha_o$, have been linked to two distinct neurologic conditions. In 2013, four children with early infantile epileptic encephalopathy were identified with mutations in *GNAO1* (Nakamura et al., 2013). Since then, a growing number of patients presenting with epilepsy and/or hyperkinetic movement disorders have been found to exhibit de novo mutations in *GNAO1* (Feng et al.,

2017, 2018). It was recognized in 2016 that some *GNAO1* mutations result in movement disorders without epilepsy (Kulkarni et al., 2016; Saitsu et al., 2016). To date, there are over 70 published cases of children with mutations in *GNAO1* presenting with early infantile epileptic encephalopathy 17 (Online Mendelian Inheritance in Man 615473) and/or neurodevelopmental disorder with involuntary movements (Online Mendelian Inheritance in Man 617493) (Nakamura et al., 2013; EuroEPINOMICS-RES Consortium et al., 2014; Law et al., 2015; Talvik et al., 2015; Ananth et al., 2016; Dhamija et al., 2016; Epi4K Consortium, 2016; Gawlinski et al., 2016; Kulkarni et al., 2016; Marcé-Grau et al., 2016; Menke et al., 2016; Saitsu et al., 2016; Yilmaz et al., 2016; Arya et al., 2017; Danti et al., 2017; Sakamoto et al., 2017; Schorling et al., 2017; Blumkin et al., 2018; Bruun et al., 2018; Gerald et al., 2018; Honey et al., 2018; Koy et al., 2018; Marecos et al., 2018; Okumura et al., 2018; Rim et al., 2018; Takezawa et al., 2018;

This work was supported by a grant from the Bow Foundation [2], Michigan State University's (MSU's) department of Comparative Medicine and Integrative Biology, and the MSU discretionary funding initiative [34149].
<https://doi.org/10.1124/jpet.119.262733>.

^S This article has supplemental material available at jpet.aspetjournals.org.

ABBREVIATIONS: BODIPY, boron-dipyrromethene; GOF, gain-of-function; gRNA, guide RNA; HEK, human embryonic kidney; PCR, polymerase chain reaction; PTZ, pentylenetetrazol; RIPA, radioimmunoprecipitation assay; ssODN, single-stranded oligodeoxynucleotide; WT, wild type.

Waak et al., 2018; Xiong et al., 2018; Kelly et al., 2019; Schirinzi et al., 2019).

More than 40 pathologic variants of *GNAO1* have been reported. Using a cell-based biochemical signaling assay, we classified many of those $G\alpha_o$ variants for their ability to inhibit cAMP production in transfected human embryonic kidney (HEK) 293 cells (Feng et al., 2017). Some mutant $G\alpha_o$ proteins were unable to support receptor-mediated inhibition of cAMP, which classifies them as having a loss-of-function mechanism in vitro. These loss-of-function mutants were associated with epilepsy (Feng et al., 2017). In contrast, mutations resulting in enhanced cAMP inhibition [gain-of-function (GOF)] or normal cAMP regulation were generally associated with movement disorders (Feng et al., 2017).

To permit mechanistic studies and preclinical drug testing, we had previously created a mouse model with a *GNAO1* GOF mutation, G203R, that was identified in patients who showed both epilepsy and movement disorders (Saitsu et al., 2016). As predicted, the *Gnao1*^{+/G203R} (G203R) mutant mice exhibited motor coordination and gait abnormalities as well as enhanced seizure susceptibility in pentylenetetrazol (PTZ) kindling studies (Feng et al., 2019). The R209H mutations are some of the most common pathogenic *GNAO1* mutations (Schirinzi et al., 2019). Patients with de novo, heterozygous R209H mutations in *GNAO1* display severe choreoathetosis and dystonia but do not exhibit seizures (Supplemental Table 1). Interestingly, the R209H mutation was found to have essentially normal function for cAMP inhibition in HEK293T cells. Despite this normal function in an in vitro assay, it causes a severe form of movement disorder in patients, often requiring intensive care unit admission (Ananth et al., 2016; Marecos et al., 2018). This discrepancy between the normal functionality in vitro and its clear clinical pathologic role makes the R209H mutation of substantial interest for in vivo physiologic studies.

We used a battery of behavioral tests to measure motor skills in heterozygous *Gnao1*^{+/R209H} mutant mice as well as PTZ kindling studies to assess seizure susceptibility. As expected, *Gnao1*^{+/R209H} mice did not show enhanced seizure susceptibility in PTZ kindling studies. Male and female *Gnao1*^{+/R209H} mice displayed significant hyperactivity in an open field assessment. This finding was surprising because mice in our previous *GNAO1*-related movement disorder model, *Gnao1*^{+/G203R}, did not show significant differences on the open field test (Feng et al., 2019). This difference in movement phenotype is consistent with the wide heterogeneity of movement patterns displayed by patients with *GNAO1* mutations (Nakamura et al., 2013; Ananth et al., 2016; Dhamija et al., 2016; Kulkarni et al., 2016; Marcé-Grau et al., 2016; Menke et al., 2016; Feng et al., 2018).

Having a mouse model with a strong movement phenotype facilitates mechanistic studies of *GNAO1* mutants, and this allowed us to begin allele-specific preclinical drug testing. The neuroleptic risperidone was reportedly beneficial in a patient with a *GNAO1* R209H mutation (Ananth et al., 2016). Here we show risperidone attenuates hyperactivity in our R209H mutant mice. This suggests risperidone or related agents may be beneficial for *GNAO1* patients with the R209H mutation.

Materials and Methods

Animals. *Gnao1*^{+/R209H} mice on a C57BL/6J background were generated in the Michigan State University Transgenic and Gene

Editing Facility (<https://tgef.vprgs.msu.edu>) as described below. Mice (8–12 weeks old) were housed on a 12-hour light/dark cycle with ad libitum access to food and water. All experiments were performed in accordance with National Institutes of Health guidelines, and protocols were approved by the Michigan State University Institutional Animal Care and Use Committee.

Generation of *Gnao1* R209H Edited Mice. Mutant *Gnao1*^{+/R209H} mice were generated via CRISPR/Cas9 genome editing on a C57BL/6J genomic background. CRISPR guide RNA (gRNA) selection and locus analysis were performed using the Benchling platform (Benchling, Inc., San Francisco, CA). A gRNA targeting exon 6 of the *Gnao1* locus (ENSMUSG00000031748) was chosen to cause a double-strand DNA break 3 bp downstream of codon R209. A single-stranded oligodeoxynucleotide (ssODN) carrying the R209H mutation CGC > CAC with short homology arms was used as a repair template (Fig. 1; Table 1). Ribonucleoprotein complexes consisting of a synthetic CRISPR RNA/trans-activating CRISPR RNA hybrid and Alt-R S.p. Cas9 Nuclease V3 protein (Integrated DNA Technologies, Inc., Coralville, IA) were used to deliver CRISPR components along with the ssODN to mouse zygotes via electroporation as previously described (Feng et al., 2017, 2019). Edited embryos were implanted into pseudo-pregnant dams using standard techniques. Resulting litters were screened by polymerase chain reaction (PCR) (Phire Green HSII PCR Mastermix, F126L; Thermo Fisher, Waltham, MA), T7 Endonuclease I assay (M0302; New England Biolabs Inc.), and Sanger sequencing (GENEWIZ, Inc., Plainfield, NJ) for edits of the target site.

Genotyping and Breeding. Studies were done on N1 R209H heterozygotes with comparisons to littermate controls. To generate *Gnao1*^{+/R209H} heterozygotes (N1 backcross), two founder *Gnao1*^{+/R209H} mice, one male and one female, were crossed with wild-type (WT) C57BL/6J mice obtained directly from The Jackson Laboratory (Bar Harbor, ME).

DNA was extracted by an alkaline method (Kehrl et al., 2014) from ear clips done before weaning. PCR products were generated with primers flanking the mutation site (Forward 5' GGACAGGTGTCACA GGGGAT 3'; 5' ACTGGCCTCCCTTGCAATA 3'), which produces a 375-bp product. Reaction conditions were: 0.8 μ l template, 4 μ l 5 \times Promega PCR buffer, 0.4 μ l 10 mM deoxyribonucleotide triphosphates, 1 μ l 10 μ M Forward Primer, 1 μ l 10 μ M Reverse Primer, 0.2 μ l Promega GoTaq, and 12.6 μ l DNase free water (catalog no. M3005; Promega, Madison, WI). Samples were denatured for 4 minutes at 95°C and then underwent 32 cycles of PCR (95°C for 30 seconds, 63°C for 30 seconds, and 72°C for 30 seconds) followed by a 7-minute final extension at 72°C. Ethanol precipitation was done on the PCR products, and then samples were sent for Sanger sequencing (GENEWIZ, Inc., Plainfield, NJ).

Behavioral Assessment. Male and female *Gnao1*^{+/R209H} mice (8–12 weeks of age) and their *Gnao1*^{+/+} littermates underwent a battery of behavioral testing to assess motor phenotype as described previously (Feng et al., 2019). Before each experiment, mice were acclimated for 10 minutes to the testing room. Experiments were performed by two female researchers. All behavioral studies were done by individuals who were blind to the genotype of the animals until completion of data collection.

Open Field. The open field test is frequently used to assess locomotion, exploration, and anxiety (Tatem et al., 2014; Seibenhener and Wooten, 2015; Feng et al., 2019). The test was conducted in Fusion VersaMax clear 42 \times 42 \times 30 cm arenas (Omnitech Electronics, Inc., Columbus, OH). *Gnao1*^{+/R209H} mice of both sexes and their littermates were placed in the arena for 30 minutes. Using the Fusion Software, we evaluated distance traveled (cm) in terms of novelty, sustained, and total movement corresponding to the first 10 minutes, 10–20 minutes, and total of 30 minutes. As a potential measure of anxiety, the fraction of time spent in the center was assessed. The center area was defined as the 20.32 \times 20.32 cm area within the middle of the arena.

Rotarod. To assess motor skills, we used the Economex accelerating RotaRod (Columbus Instruments, Columbus, OH). The protocol occurred over a 2-day period. On day 1, mice were trained for three

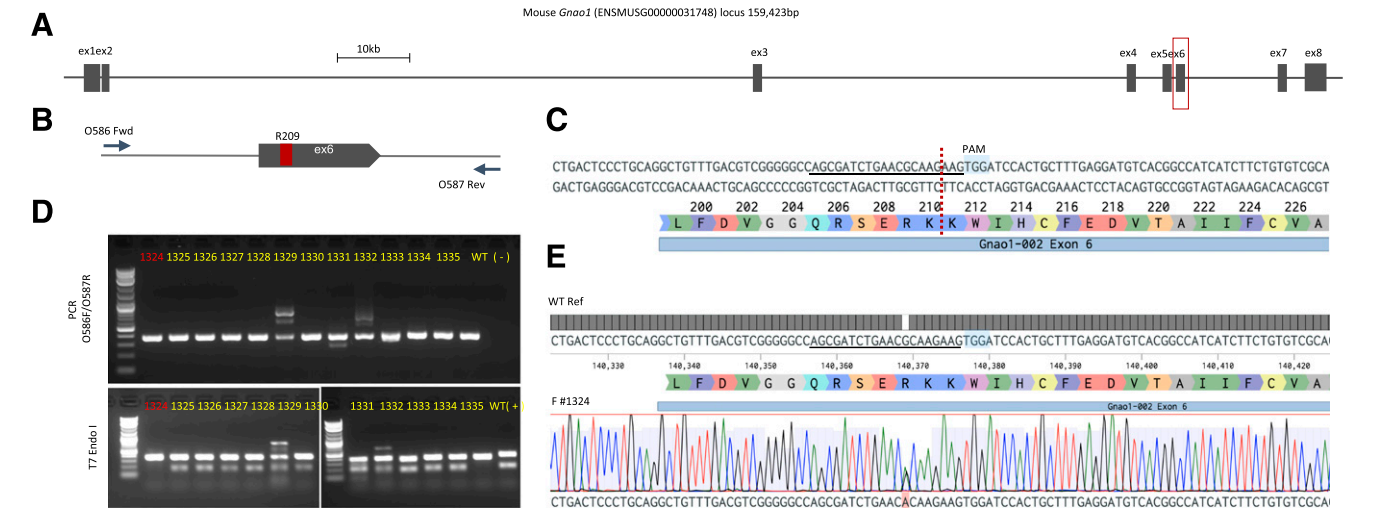


Fig. 1. Targeting of the mouse *Gnao1* locus. (A) Mouse *Gnao1* genomic locus (exon size not to scale), red outline is magnified in (B) showing exon 6 and relative location of codon 209 and PCR primers O586 and O587. (C) Location and exact sequence of gRNA target within exon 6, dotted red line denotes double-strand DNA break, protospacer-adjacent motif (PAM) is highlighted and sequence corresponding to gRNA protospacer is underlined [also in (E)]. (D) Raw gel electrophoresis images showing PCR of the target region and T7 Endonuclease I (T7 Endo I) digestion analysis of founders 1324–1335 ($n = 12$), with WT, H₂O (–), and T7Endo I (+) controls. Founder 1324 (red number) was positive for the mutation on one allele and WT on the other; note that the single bp mismatch was not reliably detected by T7 Endo I assay. (E) Exact sequence of edited founder 1324 as aligned to WT reference genome, two peaks (G and A) are detected on the sequence chromatogram, indicating the presence of both WT and edited R209H allele. Endo, endonuclease; Ex, exon; Fwd, forward; Ref, reference; Rev, reverse.

2-minute training sessions, with 10 minutes between each training trial. During the first two sessions, the RotaRod maintained a constant rotational speed of 5 rpm. The third training trial started at 5 rpm and accelerated at 0.1 rpm/s for 2 minutes. The following day, mice ran three more trials with a 10-minute break in between: two more 2-minute training trials and a final 5-minute test trial. Each of these trials started at 5 rpm with constant acceleration of 0.1 rpm/s. For all training and test trials, latency to fall off the spindle was recorded in seconds.

Grip Strength. To assess mouse grip strength, we used seven homemade weights (10, 18, 26, 34, 42, 49, and 57 g) with a 2.54-cm ring for the mouse to grasp. The mouse was held by the middle/base of the tail and lowered to the weight. Once the mouse grasped the weighted ring with its forepaws, the mouse was lifted until the weight cleared the bench. For each weight, the mouse was given up to three trials to suspend the weight above the table for 3 seconds. If cleared, the next heaviest weight was tried. If the weight was not held, the total time and maximum weight lifted were recorded, and a grip strength score was calculated from Deacon et al. (2016). The calculated score was normalized to mouse body weight, which was measured the day of the test.

DigiGait. Mouse gait analysis was performed on a DigiGait apparatus (Mouse Specifics, Inc, Framingham, MA). After acclimation, each mouse was placed on the treadmill at speeds of 18, 20, 22, 25, 28, 32, and 36 cm/s. A 10-second clip was recorded with a video camera located below the belt. There was a 5-minute rest between each speed. Recordings were analyzed with the DigiGait analysis program to assess the prespecified parameters of stride length and paw angle variability. Values for all four paws were averaged to give one value per mouse—the reported n values are the number of mice. In addition, the maximum speed at which each mouse was able to successfully complete a 10-second test after three attempts was recorded as described (Feng et al., 2019).

PTZ Kindling Study. A PTZ kindling protocol was performed as described (Kehrl et al., 2014; Feng et al., 2019) to assess mouse susceptibility to seizure induction. Mice were injected with a subconvulsive dose of PTZ (40 mg/kg, i.p.) every other day for up to 24 days, and mice then were observed for 30 minutes postdose. Kindling was defined as death or tonic-clonic seizures on two consecutive injection days, after which mice were euthanized. Kaplan-Meier survival

analysis was done based on the number of injections to achieve kindling.

Gα_o Protein Expression. Mice (6–8 weeks old) were sacrificed, and their brains were dissected into different regions and flash-frozen in liquid nitrogen. For Western blot analysis, tissues were thawed on ice and homogenized for 5 minutes with 0.50-mm zirconium beads in a Bullet Blender (Next Advance, Troy, NY) in radioimmunoprecipitation assay (RIPA) buffer (20 mM Tris-HCl, pH7.4; 150 mM NaCl; 1 mM EDTA; 1 mM β-glycerophosphate; 1% Triton X-100; and 0.1% SDS) with protease inhibitor (Roche/1 tablet in 10 ml RIPA). Sample homogenates were centrifuged for 5 minutes at 4°C at 13,000g. Supernatants were collected and protein concentrations determined using the bicinchoninic acid method (Pierce, Rockford, IL). Protein concentration was normalized for all tissues with RIPA buffer, and 2× SDS sample buffer containing β-mercaptoethanol (Sigma-Aldrich) was added. Thirty micrograms of protein was loaded onto a 12% 2-[bis(2-hydroxyethyl)amino]-2-(hydroxymethyl)propane-1,3-diol SDS-PAGE gel, and samples were separated for 1.5 hours at 160 V. Proteins were then transferred to an Immobilon-FL polyvinylidene

TABLE 1
Location and sequence of gRNA and ssODN template for CRISPR-Cas targeting *Gnao1* locus; primers and genotyping method for *Gnao1*^{+/R209H} mice

<i>Gnao1</i> R209H Chr 8: 93,950,334	
Location	
gRNA target 5' N20-PAM	5' AGCGATCTGAACGCAAGAAG TGG 3'
ssODN template (reverse complement)	GTTTCGTCCTCGTGGAGCACCTGG TCATAGCCGCTGAGTGCGACACAG AAGATGATGGCCGTGACATCCTCA AAGCAGTGGATCCACTTCTTGTGT TCAGATCGCTGGCCCCCGACGTCA AACAGCCTGCAGGGAGTCAGGGAA AGCTGTGAGGGCGGGGACGCCTA
PCR primers	O586 FWD: 5' GGACAGGTGTACACAG GGGAT 3' O587 REV: 5' ACTGGCCTC CCTTGCCAATA 3'
Genotyping	By Sanger Sequencing

Chr, chromosome; FWD, forward; PAM, protospacer-adjacent motif; REV, reverse.

difluoride membrane (Millipore, Billerica, MA) on ice either for 2 hours at 100 V, 400 mA or overnight at 30 V, 50 mA. Immediately after transfer, polyvinylidene difluoride membranes were washed and blocked in Odyssey PBS blocking buffer (LI-COR) for 40 minutes at room temperature. The membranes were then incubated with anti-G α_o (rabbit; 1:1000; sc-387; Santa Cruz biotechnologies, Santa Cruz, CA) and anti-actin (goat; 1:1000; sc-1615; Santa Cruz) antibodies diluted in Odyssey blocking buffer with 0.1% Tween-20 overnight at 4°C. Following four 5-minute washes in phosphate-buffered saline with 0.1% Tween-20, the membrane was incubated for 1 hour at room temperature with secondary antibodies (both 1:10,000; IRDye 800CW Donkey anti-rabbit; IRDye 680RD Donkey anti-goat; LI-COR Biosciences) diluted in Odyssey blocking buffer with 0.1% Tween-20. The membrane was subjected to four 5-minute washes in PBS–Tween-20 and a final rinse in PBS for 5 minutes. The membrane was kept in the dark, and the infrared signals at 680 and 800 nm were detected with an Odyssey Fc image system (LI-COR Biosciences). The G α_o polyclonal antibody recognizes an epitope located between positions 90–140 G α_o (Santa Cruz Technical Support, personal communication), so there should be no interference from the R209H mutation.

Kinetics of Nucleotide Binding. To estimate GDP release rates, which can control activation of G proteins, we measured the kinetics of binding of the fluorescent ligand 4–4-difluoro-5,7-dimethyl-4-bora-3a,4a-diaza-s-indacine-3-yl (BODIPY-FL)-GTP γ S as described previously (McEwen et al., 2002). In brief, WT and mutant His6-tagged G α_o subunits were expressed in *Escherichia coli* and purified by Ni-nitrilotriacetic acid affinity chromatography as previously described (Lee et al., 1994) and stored frozen at –80°C in 50 mM HEPES 100 mM NaCl buffer containing 50 μ M GDP to stabilize the protein. Protein was diluted to 200 nM in binding buffer (50 mM HEPES, 10 mM MgCl₂, 1 mM EDTA, and 1 mM dithiothreitol, pH 8.0), and then 100 nM BODIPY-GTP γ S was added, and fluorescence was monitored at 485 nm excitation, 510 nm emission in a Tecan Infinite M1000 Pro microplate reader at 24°C. Experiments were done on three different days each in duplicate, and results were averaged. Rate constants and $t_{1/2}$ were determined by fitting results to the equation $Y = Y_0 + (Y_{\max} - Y_0) \cdot (1 - e^{-k \cdot t})$ in GraphPad Prism v. 8, in which Y_0 was constrained to be shared between the WT and R209H mutant data sets.

Risperidone Effects on Motor Behavior. Naïve 8–12-week-old *Gnao1*^{+/R209H} and *Gnao1*^{+/+} littermates of either sex were tested for effects of risperidone on their activity in the open field arena. The study was run over 5 days: On day 1, mice underwent the open field protocol described above to establish a baseline. On day 3, mice were habituated in the experimental room for 10 minutes and then given a single intraperitoneal dose of 2.0 mg/kg risperidone (Cayman Chemical, Ann Arbor, MI) or vehicle control. Risperidone was dissolved in DMSO at a concentration of 5 mg/ml, and further dilutions were done in deionized water. Thirty minutes following injection, mice were placed in the open field arena for a 30-minute testing time. On day 5, mice were retested in the same open field protocol without injection to assess drug washout. A week later, the same protocol was followed to test the effects an intraperitoneal dose of 0.5 mg/kg risperidone had on the WT and R209H mice.

Statistical Analysis. Data were analyzed with unpaired Student's *t* test or Mantel-Cox and two-way ANOVA with Bonferroni corrections as appropriate using GraphPad Prism 7.0 (GraphPad, La Jolla, CA). A *P* < 0.05 was considered the cutoff for significance throughout. Detailed discussion of statistical analyses can be found within figure legends.

Results

***Gnao1*^{+/R209H} Mice Are Produced at the Expected Frequency and Have Normal Viability.** Two founder *Gnao1*^{+/R209H} mice, one male and one female, were crossed

with C57BL/6J mice. Out of 98 offspring of a cross of *Gnao1*^{+/R209H} with WT mice, 51 heterozygotes and 47 WT were observed. *Gnao1*^{+/R209H} mice exhibit no overt postural or movement abnormalities or seizures under normal housing conditions. Adult mice showed no statistically significant differences in weight between WT and *Gnao1*^{+/R209H} genotypes of either sex.

Both Male and Female *Gnao1*^{+/R209H} Show Significant Hyperactivity in the Open Field Arena but No Significant Differences on the Rotarod or Grip Strength Test. Patients with R209H mutations present with hyperkinetic movement disorders (Ananth et al., 2016; Dhamija et al., 2016; Menke et al., 2016). To detect motor abnormalities, *Gnao1*^{+/R209H} mice were subjected to a battery of behavioral tests. The open field arena was used to test overall locomotor activity. We divided the test into two sections reflecting activity in a novel environment (0–10 minutes) and then sustained activity (10–30 minutes). *Gnao1*^{+/R209H} mice of both sexes showed markedly increased activity in the sustained activity period compared with their wild-type littermates (Fig. 2B). Females also had significantly increased activity in the first 10 minutes (novelty period, Fig. 2B). As a potential indicator of anxiety-like behavior, male and female *Gnao1*^{+/R209H} mice also displayed reduced time in center (Fig. 2, A and B).

An accelerating RotaRod test was used to assess motor coordination and balance. Neither male nor female *Gnao1*^{+/R209H} mice displayed impaired performance (Fig. 2C). Also, grip strength showed no differences between *Gnao1*^{+/R209H} and wild-type littermates of either sex (Fig. 2D).

Male *Gnao1*^{+/R209H} Mice Display a Modestly Reduced Stride Length. Gait patterns were assessed using DigiGait analysis. Male *Gnao1*^{+/R209H} mice (Fig 3, B) showed a highly significant genotype effect with reduced stride length compared with wild-type littermates (*P* < 0.001, two-way ANOVA), but the magnitude of the effect was modest (5.6% decrease averaged across all speeds). In posttest analysis, only the top speed (36 cm/s) reached significance individually (*P* < 0.01). Female *Gnao1*^{+/R209H} mice did not show significant differences in stride length from WT (Fig. 3, A). However, as previously reported for G203R mutant mice, the female *Gnao1*^{+/R209H} showed a significantly reduced maximum run speed on the treadmill (Fig. 3E *P* < 0.01, *t* test). This was not due to reduced body size because length, as detected by the DigiGait system (WT 9.54 cm: vs. R209H 10.17 cm), and weights were not significantly different. There was no significant difference in paw angle variability for either males or females. All parameters of DigiGait analysis are shown in Supplemental Tables 3 and 4, and false discovery rate calculation probed of significantly different parameters from the DigiGait data in *Gnao1*^{+/R209H} mice is shown in Supplemental Fig. 2.

***Gnao1*^{+/R209H} Mice Are Not Sensitive to PTZ Kindling.** Repeated application of a subthreshold convulsive stimulus leads to the generation of full-blown convulsions in a process called kindling (Dhir, 2012). *GNAO1* variants differ in their ability to cause epileptic seizures in patients. Those carrying the R209H mutant allele do not exhibit a seizure disorder (Ananth et al., 2016; Kulkarni et al., 2016; Menke et al., 2016). In accordance with the patients' pattern, *Gnao1*^{+/R209H} mice did not show increased susceptibility to

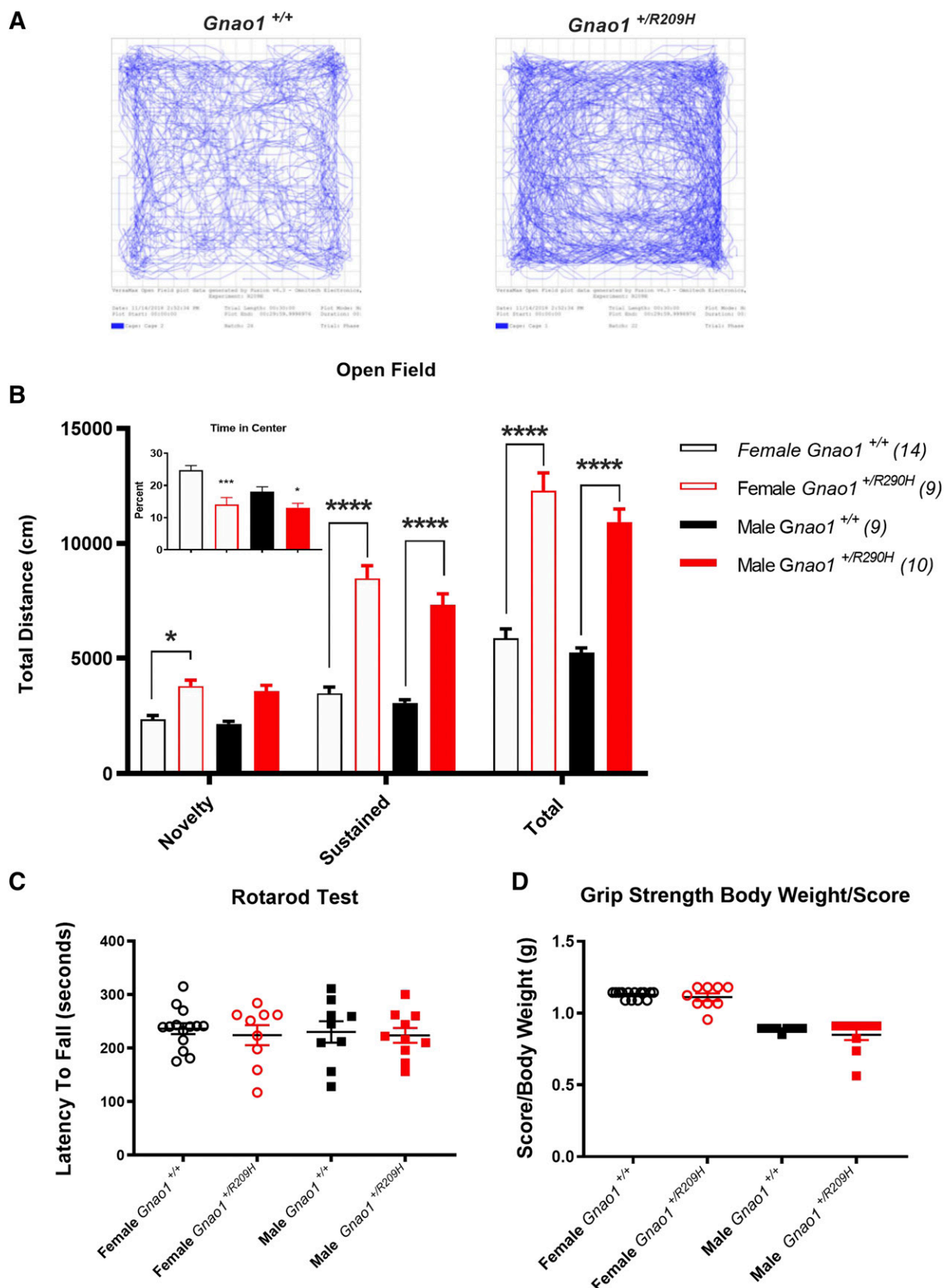


Fig. 2. *Gnao1*^{+/R209H} mice show significant hyperactivity and reduced time in center in the open field arena. (A) Representative heat maps of *Gnao1*^{+/R209H} mice and *Gnao1*^{+/+} mice in the open field arena. (B) Time spent in the open field arena was separated into 0–10 minutes (novelty) and 10–30 minutes (sustained). *Gnao1*^{+/R209H} male and female mice exhibit increased locomotion in the novelty period. Hyperactivity observed in the sustained period and for total travel time (two-way ANOVA; **P* < 0.05; ****P* < 0.001; *****P* < 0.0001). Female R209H mutant mice also showed significantly greater distance traveled in the novelty period (**P* < 0.05). *Gnao1*^{+/R209H} mice of both sexes spend less time in center areas of the open field arena compared with wild-type littermates. (C) Neither male nor female *Gnao1*^{+/R209H} mice show significant differences on the RotaRod. (D) There is also no significant difference in grip strength between wild-type and *Gnao1*^{+/R209H} mice. Data are shown as mean ± S.E.M.

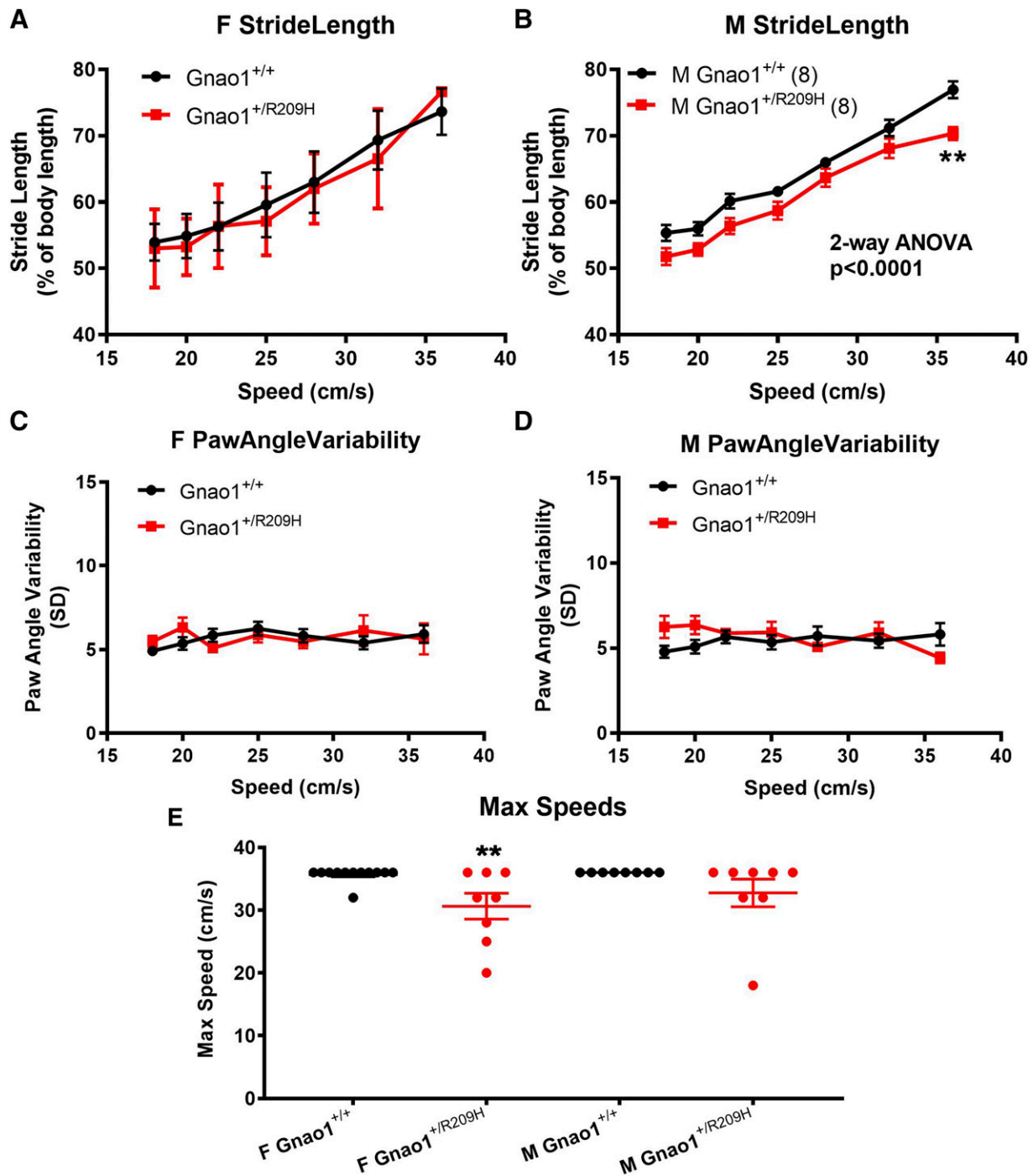


Fig. 3. Male and female *Gnao1*^{+/R209H} mice shows gait abnormalities in different tests on the DigiGait imaging system. (B) Male *Gnao1*^{+/R209H} mice showed reduced stride length compared with wild-type littermates (two-way ANOVA with Bonferroni multiple comparison posttest), whereas female *Gnao1*^{+/R209H} mice showed a normal stride length. (A) Neither male nor female *Gnao1*^{+/R209H} exhibited significant differences in paw angle variability (C and D) compared with wild-type littermates. (E) At speeds greater than 25 cm/s, female *Gnao1*^{+/R209H} had a reduced ability to run on the treadmill. F, female; M, male. ** P < 0.01.

kindling-induced seizures (Fig. 4). This contrasts with our previous report of increased kindling sensitivity in male G203R and female G184S mutant mice (Kehrl et al., 2014; Dhamija et al., 2016; Feng et al., 2019).

***Gnao1*^{+/R209H} Mice Have Normal $G\alpha_o$ Protein Expression in the Brain.** To understand why R209H mutant mice do not show a phenotypic difference in the kindling test while G203R mutants do, we assessed $G\alpha_o$ protein expression levels.

Cortex, hippocampus, striatum, cerebellum, brain stem, and olfactory bulb were harvested and homogenized to measure the effect of the R209H mutation on $G\alpha_o$ protein expression. Western blots showed no difference in $G\alpha_o$ protein expression between WT and *Gnao1*^{+/R209H} mice in any of the measured brain regions (Fig. 5, A and B). This is consistent with our previous analysis of protein expression in HEK293T cells with transiently transfected $G\alpha_o$ R209H plasmid (Feng et al.,

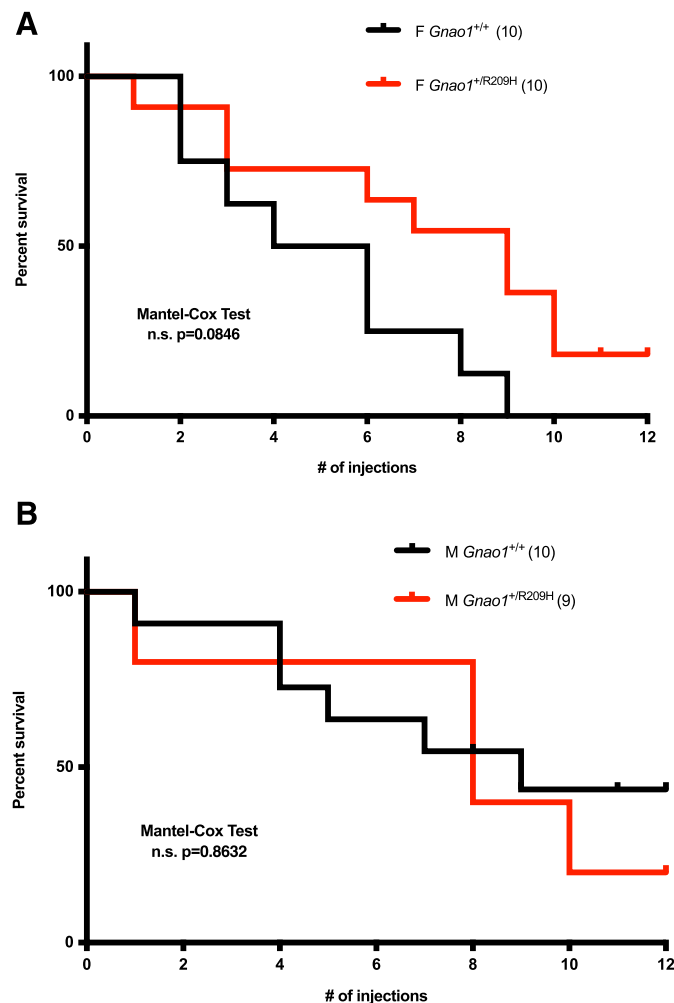


Fig. 4. *Gnao1*^{+/R209H} mice do not have an enhanced PTZ kindling response. (A and B) Neither male nor female *Gnao1*^{+/R209H} mice showed significant differences in sensitivity to PTZ injection compared with wild-type littermates (n.s. Mantel-Cox test). F, female; M, male; n.s., not significant.

2017). The normal expression of the R209H mutant contrasts with the reduced expression of $G\alpha_o$ in brains of $G\alpha_o$ ^{+/G203R} mutant mice (Feng et al., 2019).

Kinetics of Nucleotide Binding to Mutant $G\alpha_o$. Both patients and mice heterozygous for the $G\alpha_o$ R209H mutation display movement phenotypes; however, the mutant $G\alpha_o$ supports normal cAMP regulation in the cell-based cAMP assay (Feng et al., 2017). To consider possible mechanisms for this discrepancy, we measured the rate of GDP release from mutant $G\alpha_o$ using the BODIPY-GTP γ S binding kinetics method (McEwen et al., 2002). The rate of GTP γ S binding to WT $G\alpha_o$ was slow ($T_{1/2}$ 1261 seconds, Fig. 5C), as expected. The R209H mutant $G\alpha_o$ showed markedly faster binding of BODIPY-GTP γ S ($T_{1/2}$ 203 seconds 6.2 \times faster than WT, Fig. 5, C and D), suggesting a faster rate of GDP release. In addition to the faster rate of binding, the amplitude of binding was lower for the R209H mutant. Though this lower amplitude of binding might be due to either a lower affinity of the mutant for the BODIPY-GTP γ S or to instability under the binding conditions, we do show that the R209H mutant definitely does have abnormal interactions with nucleotides—GDP and/or GTP.

Risperidone Treatment Attenuated the Hyperactivity of *Gnao1*^{+/R209H} Mice. Patients with *GNAO1* mutations were tried on multiple drugs to alleviate motor symptoms (Supplemental Table 1). Risperidone, an atypical antipsychotic drug, showed beneficial effects in one of the patients. It has also been effective in drug-induced dyskinesia (Carvalho et al., 2003). We show that *Gnao1*^{+/R209H} mice exhibit complete abrogation of movement at 2 mg/kg risperidone, which recovered upon retesting 2 days later (Fig. 6, A and C). WT mice also show a significant decrease in locomotion after 2 mg/kg risperidone treatment (Fig. 6A). After a single 0.5 mg/kg dose of risperidone, both WT and *Gnao1*^{+/R209H} mice exhibit a decrease in locomotion compared with vehicle-treated littermates (Fig. 6B). As expected, hyperactivity of mutant mice was observed during baseline testing on day 1, and the hyperactivity had returned on day 5 following the 2-day washout period after the risperidone doses (Fig. 6C). Neither 2.0 mg/kg nor 0.5 mg/kg selectively affected *Gnao1*^{+/R209H}, as assessed by percent suppression of distance traveled (Supplemental Fig. 1).

Discussion

We have developed a novel mouse model carrying an R209H mutation in the *Gnao1* gene that leads to a serious movement disorder (Ananth et al., 2016; Dhamija et al., 2016). Though *GNAO1* mutations are rare in humans, the R209H mutation is the second most common found in patients with *GNAO1*-related disorders. The mice have a clear movement phenotype confirming the pathologic nature of this mutation despite earlier work showing that it could normally support receptor-mediated regulation of cAMP in HEK cells (Feng et al., 2017). This model will provide a powerful tool to both understand neural mechanisms of the dysfunction of the R209H $G\alpha_o$ protein as well as permit preclinical drug repurposing studies.

The goal of personalized medicine is to define treatments for an individual patient. Knowing which gene is involved is beneficial, but different mutant alleles, even in the same gene, can produce quite distinct effects. Here we report a second mouse model of *GNAO1*-related neurologic abnormalities. The *Gnao1* R209H mutant mice display motor abnormalities but no seizures, which differs from our previous *Gnao1* G203R mouse model (Feng et al., 2019). This is consistent with the clinical pattern of patients with *GNAO1* R209H, who present with neurodevelopmental delay with involuntary movements without seizures (Ananth et al., 2016; Dhamija et al., 2016).

The specific movement abnormalities seen with the *Gnao1* R209H mutant mice were somewhat unexpected; our previous mouse model, *Gnao1*^{+/G203R}, showed significant motor impairments in RotaRod and DigiGait but had no changes in the open field test (Feng et al., 2019). In contrast, the *Gnao1* R209H mutant mice reported here have profound hyperactivity in the open field test and either no or only modest deficits in RotaRod and DigiGait analysis. Patients with the G203R or R209H mutations both display movement disorder, with choreoathetosis and dystonia as the most common patterns (Saito et al., 2016; Feng et al., 2018). Interestingly, patients with the R209H mutation have somewhat more choreoathetosis compared with those with the G203R mutation, although they display similar frequencies of dystonia (Feng et al., 2018). Such differences in patient phenotype may relate to the

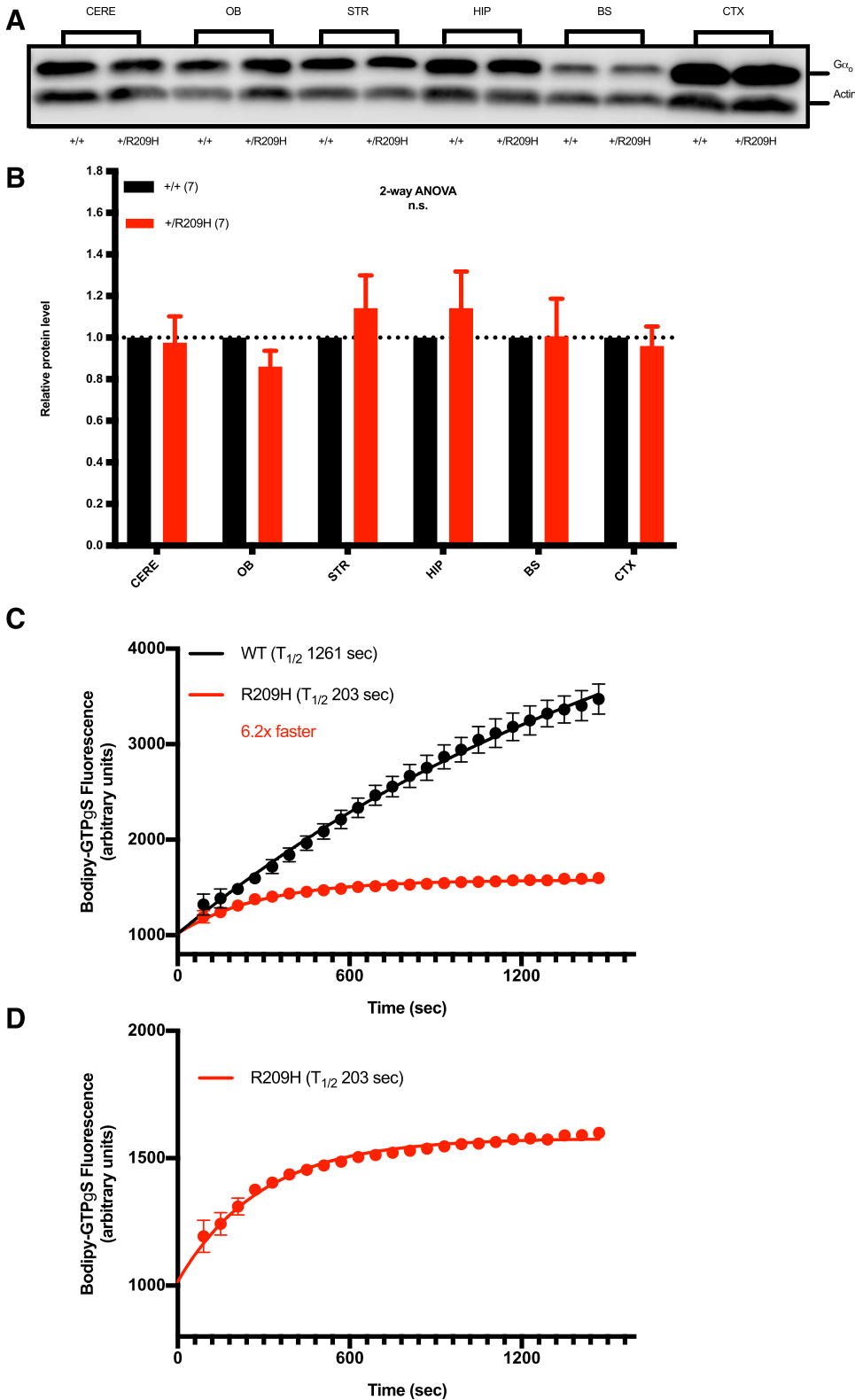


Fig. 5. Biochemical analysis of brain $G\alpha_o$ protein levels and in vitro nucleotide exchange for WT and R209H mutant $G\alpha_o$. (A) Brain regions (cortex, hippocampus, striatum, cerebellum, brain stem, and olfactory bulb homogenates) from WT and *Gnao1*^{+R209H} mice were assessed by Western blot for levels of $G\alpha_o$ protein. (B) Protein levels of *Gnao1*^{+R209H} brain samples were quantified using LI-COR IRDye staining, and values were normalized to actin levels and then to the control sample from WT run on the same day. There was no significant difference in any of the regions between WT and mutant mice ($n = 7$). (C and D) The kinetics of BODIPY-FL-GTPγS binding were measured as described in *Materials and Methods*. The time course of the fluorescence increase was fit to an exponential function (connecting lines) and the $T_{1/2}$ calculated from the rate constant of the exponential function (see *Materials and Methods*). Nucleotide binding experiments were performed in duplicate, and results from the separate days were averaged. Error bars and mean \pm S.D. ($n = 3$). For some data points, error bars are smaller than the symbol and are not shown. BS, brain stem; CERE, cerebellum; CTX, cortex; HIP, hippocampus; n.s., not significant; OB, olfactory bulb; STR, striatum; $T_{1/2}$, half-time; WT, wild-type.

differences in the animal models' behavior. In looking at the behavior of the R209H model specifically, the striking hyperactivity of the male R209H mutant mice points to increased dopamine signaling in the striatum as a possible mechanism. Suppression of that hyperactivity with risperidone is consistent with that mechanism.

The two movement disorder-associated *GNAO1* mutations R209H and G203R also have different patterns in in vitro studies of cAMP regulation in HEK293T cells (Feng et al., 2017). Interestingly, the $G\alpha_o$ R209H mutant supports normal cAMP regulation and is expressed at normal levels both in HEK cells (Feng et al., 2017) and in the brain (this study).

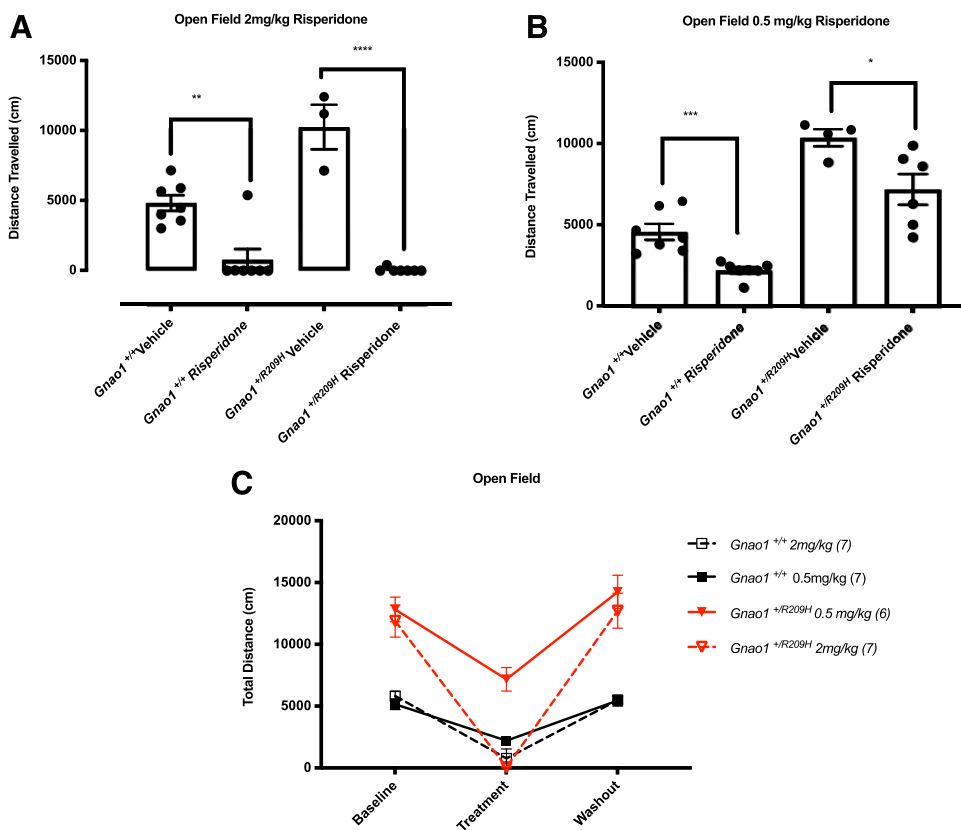


Fig. 6. Risperidone treatments decrease hyperkinetic movements in *Gnao1*^{+/R209H}. (A) *Gnao1*^{+/R209H} mice show complete abrogation of movement compared with vehicle-treated *Gnao1*^{+/R209H} littermates following a 2.0 mg/kg dose of risperidone. Student's unpaired *t* test. (B) At 0.5 mg/kg, both WT and *Gnao1*^{+/R209H} exhibit a significant decrease in locomotion compared with vehicle controls. Student's unpaired *t* test. Wild-type mice also show a decrease in locomotion after 0.5 mg/kg risperidone treatment. (C) Comparison of 2.0 and 0.5 mg/kg treatment in WT and *Gnao1*^{+/R209H} mice. Hyperactivity of *Gnao1*^{+/R209H} mice was observed during baseline testing and recovered following the 2-day risperidone washout. **P* < 0.05; ***P* < 0.01; ****P* < 0.001; *****P* < 0.0001

In contrast, the G203R mutant is expressed at lower levels both in HEK cells (Feng et al., 2017) and in the mouse brain (Feng, H. Unpublished doctoral dissertation). Despite lower expression, it signals more strongly (GOF) in the HEK cell assay.

We also present two new pieces of information that provide insights into the pathogenicity of the R209H mutant $G\alpha_o$, despite its normal function in the HEK cell cAMP assay. Using a fluorescent nucleotide exchange assay with pure R209H mutant $G\alpha_o$, we demonstrate that the rate of binding of the GTP analog is $\sim 6.2\times$ faster than that of WT. This is typical for many hyperactive G protein mutants, since GDP release is the rate-limiting step for activation. Indeed, receptors enhance GDP release rates to activate the G protein (Iiri et al., 1994; Leyme et al., 2014; Toyama et al., 2017). Constitutive activation of $G\alpha_o$ by the R209H mutant could lead to enhanced signaling in the indirect pathway, D2 dopamine receptor neurons in striatum. The striatum is a site of substantial $G\alpha_o$ expression, and enhanced $G\alpha_o$ signaling could contribute to the hyperactivity phenotype seen in our studies. More detailed mechanistic studies of striatal neurons will be needed to further elucidate the downstream signaling mechanisms protein (e.g., ion channels, synaptic vesicle release, or neurite outgrowth) engaged by the mutant G_o in these mice and in patients.

Effective treatments are a key goal, as patients with the R209H mutation experience repeated hospitalizations (Ananth et al., 2016; Marecos et al., 2018; Schirizzi et al., 2019). Deep brain stimulation in the internal globus pallidus has proven effective in patients with *GNAO1* in attenuating the movement disorder (Kulkarni et al., 2016; Yilmaz et al., 2016; Honey et al., 2018; Koy et al., 2018). However, that invasive treatment is reserved for patients who are refractory. Risperidone is one of the oral treatments that has proven to be

beneficial, specifically in a patient with the R209H mutation (Ananth et al., 2016). Risperidone is an atypical neuroleptic that antagonizes D₂ and 5-HT receptors. $G\alpha_o$ couples to myriad G protein-coupled receptors, including the dopamine D₂ receptor, which is involved in movement control (Neve et al., 2004). In our study, risperidone was able to significantly decrease the hyperlocomotion seen in our *Gnao1*^{+/R209H} mouse model. At both the 0.5 and 2.0 mg/kg doses of risperidone, hyperactivity was attenuated in our R209H mouse model. However, this response was not selective for the *Gnao1*^{+/R209H} mutant mice because the WT mice also displayed a significant decrease in locomotion. This outcome suggests that risperidone treatment may be effective in repressing global movement while not specifically targeting a *Gnao1* R209H mechanism.

The new mouse model described here should provide a valuable tool for future mechanistic studies of *GNAO1* encephalopathies. The fact that the mouse had very distinct behavioral changes compared with our previous *Gnao1* mutant mouse models (R209H and G184S) indicates that it is very important to consider the mutant allele as well as the mutant gene in considering genetic disorders and personalized therapies.

Acknowledgments

The authors thank Dr. Michelle Mazei-Robison for her advice on organizing the behavioral battery experiments on our mutant mouse models.

Authorship Contributions

Participated in research design: Larrivee, Feng, Shaw.

Conducted experiments: Larrivee, Feng, Quinn, Shaw, Leipprandt.

Contributed new reagents or analytic tools: Demireva, Xie.

Performed data analysis: Larrivee, Feng, Shaw.

Wrote or contributed to the writing of the manuscript: Larrivee, Feng, Demireva, Neubig.

References

- Ananth AL, Robichaux-Viehoever A, Kim YM, Hanson-Kahn A, Cox R, Enns GM, Strober J, Willing M, Schlaggar BL, Wu YW, et al. (2016) Clinical Course of Six Children With GNAO1 Mutations Causing a Severe and Distinctive Movement Disorder. *Pediatr Neurol* **59**:81–84.
- Arya R, Spaeth C, Gilbert DL, Leach JL, and Holland KD (2017) GNAO1-associated epileptic encephalopathy and movement disorders: c.607G>A variant represents a probable mutation hotspot with a distinct phenotype. *Epileptic Disord* **19**:67–75.
- Blumkin L, Lerman-Sagie T, Westenberg A, Ben-Pazi H, Zerem A, Yosovich K, and Lev D (2018) Multiple Causes of Pediatric Early Onset Chorea-Clinical and Genetic Approach. *Neuropediatrics* **49**:246–255.
- Bruun TUJ, DesRoches CL, Wilson D, Chau V, Nakagawa T, Yamasaki M, Hasegawa S, Fukao T, Marshall C, and Mercimek-Andrews S (2018) Prospective cohort study for identification of underlying genetic causes in neonatal encephalopathy using whole-exome sequencing. *Genet Med* **20**:486–494.
- Carvalho RC, Silva RH, Abílio VC, Barbosa PN, and Frussa-Filho R (2003) Antidyskinetic effects of risperidone on animal models of tardive dyskinesia in mice. *Brain Res Bull* **60**:115–124.
- Danti FR, Galosi S, Romani M, Montomoli M, Carss KJ, Raymond FL, Parrini E, Bianchini C, McShane T, Dale RC, et al. (2017) GNAO1 encephalopathy: broadening the phenotype and evaluating treatment and outcome. *Neurol Genet* **3**:e143.
- Deacon RM, Nielsen S, Leung S, Rivas G, Cubitt T, Monds LA, Ezard N, Larance B, and Lintzeris N (2016) Alprazolam use and related harm among opioid substitution treatment clients - 12 months follow up after regulatory rescheduling. *Int J Drug Policy* **36**:104–111.
- Dhamija R, Mink JW, Shah BB, and Goodkin HP (2016) GNAO1-associated movement disorder. *Mov Disord Clin Pract (Hoboken)* **3**:615–617.
- Dhir A (2012) Pentylenetetrazol (PTZ) kindling model of epilepsy. *Curr Protoc Neurosci* **Chapter 9**, p Unit9.37.
- Epi4K Consortium (2016) De novo mutations in SLC1A2 and CACNA1A are important causes of epileptic encephalopathies. *Am J Hum Genet* **99**:287–298.
- EuroEPINOMICS-RES Consortium; Epilepsy Phenome/Genome Project; Epi4K Consortium (2014) De novo mutations in synaptic transmission genes including DNMI1 cause epileptic encephalopathies. *Am J Hum Genet* **95**:360–370.
- Feng H, Khalil S, Neubig RR, and Sidiropoulos C (2018) A mechanistic review on GNAO1-associated movement disorder. *Neurobiol Dis* **116**:131–141.
- Feng H, Larrivee CL, Demireva EY, Xie H, Leipprandt JR, and Neubig RR (2019) Mouse models of GNAO1-associated movement disorder: allele- and sex-specific differences in phenotypes. *PLoS One* **14**:e0211066.
- Feng H, Sjögren B, Karaj B, Shaw V, Gezer A, and Neubig RR (2017) Movement disorder in GNAO1 encephalopathy associated with gain-of-function mutations. *Neurology* **89**:762–770.
- Gawliński P, Posmyk R, Gambin T, Sielicka D, Chorazy M, Nowakowska B, Jhanganji SN, Muzny DM, Bekiesinska-Figatowska M, Bal J, et al. (2016) PEHO syndrome may represent phenotypic expansion at the severe end of the early-onset encephalopathies. *Pediatr Neurol* **60**:83–87.
- Gerald B, Ramsey K, Belpap N, Szelinger S, Siniard AL, Balak C, Russell M, Richholt R, De Both M, Claassen AM, et al. (2018) Neonatal epileptic encephalopathy caused by de novo GNAO1 mutation misdiagnosed as atypical Rett syndrome: cautions in interpretation of genomic test results. *Semin Pediatr Neurol* **26**:28–32.
- Honey CM, Malhotra AK, Tarailo-Graovac M, van Karnebeek CDM, Horvath G, and Sulistyanto A (2018) GNAO1 mutation-induced pediatric dystonic storm rescue with pallidal deep brain stimulation. *J Child Neurol* **33**:413–416.
- Iiri T, Herzmark P, Nakamoto JM, van Dop C, and Bourne HR (1994) Rapid GDP release from Gs alpha in patients with gain and loss of endocrine function. *Nature* **371**:164–168.
- Kehrl JM, Sahaya K, Dalton HM, Charbeneau RA, Kohut KT, Gilbert K, Pelz MC, Parent J, and Neubig RR (2014) Gain-of-function mutation in *Gnao1*: a murine model of epileptiform encephalopathy (EIEE17)? *Mamm Genome* **25**:202–210.
- Kelly M, Park M, Mihalek I, Rochtus A, Gramm M, Pérez-Palma E, Axeen ET, Hung CY, Olson H, Swanson L, et al.; Undiagnosed Diseases Network (2019) Spectrum of neurodevelopmental disease associated with the GNAO1 guanosine triphosphate-binding region. *Epilepsia* **60**:406–418.
- Koy A, Cirak S, Gonzalez V, Becker K, Roujeau T, Milesi C, Baleine J, Cambonie G, Boularan A, Greco F, et al. (2018) Deep brain stimulation is effective in pediatric patients with GNAO1 associated severe hyperkinesia. *J Neurol Sci* **391**:31–39.
- Kulkarni N, Tang S, Bhardwaj R, Bernes S, and Grebe TA (2016) Progressive movement disorder in brothers carrying a GNAO1 mutation responsive to deep brain stimulation. *J Child Neurol* **31**:211–214.
- Law C-Y, Chang ST, Cho SY, Yau EK, Ng GS, Fong NC, and Lam CW (2015) Clinical whole-exome sequencing reveals a novel missense pathogenic variant of GNAO1 in a patient with infantile-onset epilepsy. *Clin Chim Acta* **451** (Pt B):292–296.
- Lee E, Linder ME, and Gilman AG (1994) Expression of G-protein alpha subunits in *Escherichia coli*. *Methods Enzymol* **237**:146–164.
- Leyme A, Marivin A, Casler J, Nguyen LT, and Garcia-Marcos M (2014) Different biochemical properties explain why two equivalent Gα subunit mutants cause unrelated diseases. *J Biol Chem* **289**:21818–21827.
- Marcé-Grau A, Dalton J, López-Pisón J, García-Jiménez MC, Monge-Galindo L, Cuenca-León E, Giraldo J, and Macaya A (2016) GNAO1 encephalopathy: further delineation of a severe neurodevelopmental syndrome affecting females. *Orphanet J Rare Dis* **11**:38.
- Marecos C, Duarte S, Alonso I, Calado E, and Moreira A (2018) GNAO1: a new gene to consider on early-onset childhood dystonia. *Rev Neurol* **66**:321–322.
- McEwen DP, Gee KR, Kang HC, and Neubig RR (2002) Fluorescence approaches to study G protein mechanisms. *Methods Enzymol* **344**:403–420.
- Menke LA, Engelen M, Alders M, Odekerken VJ, Baas F, and Cobben JM (2016) Recurrent GNAO1 mutations associated with developmental delay and a movement disorder. *J Child Neurol* **31**:1598–1601.
- Nakamura K, Kodera H, Akita T, Shiina M, Kato M, Hoshino H, Terashima H, Osaka H, Nakamura S, Tohyama J, et al. (2013) De Novo mutations in GNAO1, encoding a Gαo subunit of heterotrimeric G proteins, cause epileptic encephalopathy. *Am J Hum Genet* **93**:496–505.
- Neve KA, Seamans JK, and Trantham-Davidson H (2004) Dopamine receptor signaling. *J Recept Signal Transduct Res* **24**:165–205.
- Okumura A, Maruyama K, Shibata M, Kurahashi H, Ishii A, Numoto S, Hirose S, Kawai T, Iso M, Kataoka S, et al. (2018) A patient with a GNAO1 mutation with decreased spontaneous movements, hypotonia, and dystonic features. *Brain Dev* **40**:926–930.
- Rim JH, Kim SH, Hwang IS, Kwon SS, Kim J, Kim HW, Cho MJ, Ko A, Youn SE, Kim J, et al. (2018) Efficient strategy for the molecular diagnosis of intractable early-onset epilepsy using targeted gene sequencing. *BMC Med Genomics* **11**:6.
- Saitsu H, Fukai R, Ben-Zeev B, Sakai Y, Mimaki M, Okamoto N, Suzuki Y, Monden Y, Saito H, Tziperman B, et al. (2016) Phenotypic spectrum of GNAO1 variants: epileptic encephalopathy to involuntary movements with severe developmental delay. *Eur J Hum Genet* **24**:129–134.
- Sakamoto S, Monden Y, Fukai R, Miyake N, Saito H, Miyauchi A, Matsumoto A, Nagashima M, Osaka H, Matsumoto N, et al. (2017) A case of severe movement disorder with GNAO1 mutation responsive to topiramate. *Brain Dev* **39**:439–443.
- Schirizzi T, Garone G, Travaglini L, Vasco G, Galosi S, Rios L, Castiglioni C, Barassi C, Battaglia D, Gambardella ML, et al. (2019) Phenomenology and clinical course of movement disorder in GNAO1 variants: results from an analytical review. *Parkinsonism Relat Disord* **61**:19–25.
- Schorling DC, Dietel T, Evers C, Hinderhofer K, Korinthenberg R, Ezzo D, Bönemann CG, and Kirschner J (2017) Expanding phenotype of de novo mutations in GNAO1: four new cases and review of literature. *Neuropediatrics* **48**:371–377.
- Seibenhener ML and Wooten MC (2015) Use of the Open Field Maze to measure locomotor and anxiety-like behavior in mice. *J Vis Exp* e52434.
- Takezawa Y, Kikuchi A, Haginoya K, Niihori T, Numata-Uematsu Y, Inui T, Yamamura-Suzuki S, Miyabayashi T, Anzai M, Suzuki-Muromoto S, et al. (2018) Genomic analysis identifies masqueraders of full-term cerebral palsy. *Ann Clin Transl Neurol* **5**:538–551.
- Talvik I, Möller RS, Vaheer M, Vaheer U, Larsen LH, Dahl HA, Ilves P, and Talvik T (2015) Clinical phenotype of de novo GNAO1 mutation: case report and review of literature. *Child Neurology Open* **2**:2329048X15583717.
- Tatem KS, Quinn JL, Phadke A, Yu Q, Gordish-Dressman H, and Nagaraju K (2014) Behavioral and locomotor measurements using an open field activity monitoring system for skeletal muscle diseases. *J Vis Exp* 51785.
- Toyama Y, Kano H, Mase Y, Yokogawa M, Osawa M, and Shimada I (2017) Dynamic regulation of GDP binding to G proteins revealed by magnetic field-dependent NMR relaxation analyses. *Nat Commun* **8**:14523.
- Waak M, Mohammad SS, Coman D, Sinclair K, Copeland L, Silburn P, Coyne T, McGill J, O'Regan M, Selway R, et al. (2018) GNAO1-related movement disorder with life-threatening exacerbations: movement phenomenology and response to DBS. *J Neurol Neurosurg Psychiatry* **89**:221–222.
- Xiong J, Peng J, Duan HL, Chen C, Wang XL, Chen SM, and Yin F (2018) Recurrent convulsion and pulmonary infection complicated by psychomotor retardation in an infant. *Zhongguo Dang Dai Er Ke Za Zhi* **20**:154–157.
- Yilmaz S, Turhan T, Ceylaner S, Gökben S, Tekgul H, and Serdaroglu G (2016) Excellent response to deep brain stimulation in a young girl with GNAO1-related progressive choreoathetosis. *Childs Nerv Syst* **32**:1567–1568.

Address correspondence to: Dr. Richard R. Neubig, Michigan State University, 1355 Bogue Street, B440 Life Science Building, East Lansing, MI 48824. E-mail: rneubig@msu.edu

Mice with *GNAO1* R209H Movement Disorder Variant Display Hyperlocomotion Alleviated by Risperidone

Authors: Larrivee, Casandra L.^{1,2,} Feng, Huijie ², Quinn, Josiah A. ², Shaw, Vincent, S.
², Leipprandt, Jeffrey R. ², Demireva, Elena Y.³, Xie, Huirong ³ , and Neubig, Richard R.

Journal of Pharmacology and Experimental Therapeutics

Supplemental Materials

Table Legend

Supplemental Table 1. <i>GNAO1</i> R209H Patient Classification.....	2
Supplemental Table 2. Gait analysis parameters of female <i>Gnao1</i> R209H mutant mice	3
Supplemental Table 3. Gait analysis parameters of male <i>Gnao1</i> R209H mutant mice..	4

Figure Legend

Supplemental Figure 1. WT and <i>Gnao1</i> ^{+/R209H} mice show no difference in percent suppression of locomotion after risperidone treatment	5
Supplemental Figure 2. False discovery rate (FDR) calculation probed of significantly different parameters from the DigiGait data in <i>Gnao1</i> ^{+/R209H} mice.....	6

Supplemental Table 1. *GNAO1* R209H Patient Classification

Patient No.	Sex	Amino Acid Change	Age of Onset	Presence of Epilepsy	Movement Disorder	Treatment	Motor Delay(MDD)/Intellectual Delay(ID)	Reference
1	M	R209H	17 mo	-	Chorea	DBS	MDD	Kulkarni et. al (2016)
2	M	R209H	2 y	-	Chorea	DBS	MDD	Kulkarni et. al (2016)
3	M	R209H	3 y	-	Chorea	Risperidone, BZD	MDD/ID	Anath et. al (2016)
4	M	R209H	1 y		Chorea	NA	MDD/ID	Menke et al (2016)
5	M	R209H	10 mo	-	Chorea Dystonia	TBZ, THP	MDD/NA	Dhamija et al (2016)
6	M	R209H	15 mo	-	Chorea, Dystonia	DBS	MDD/ID	Marecos et al (2018)
7	F	R209H	6 mo	-	Dystonia	NA	MDD/MID	Kelly et al (2018)
8*	F	R209C	NA	NA	Chorea	NA	MDD/ID	Saitsu et al (2016)
9*	F	R209G	3 y	-	Chorea	None	MDD/ID	Anath et al (2016)
10*	M	R209L	2 y	-	Chorea	NA	MDD/ID	Menke et al (2016)

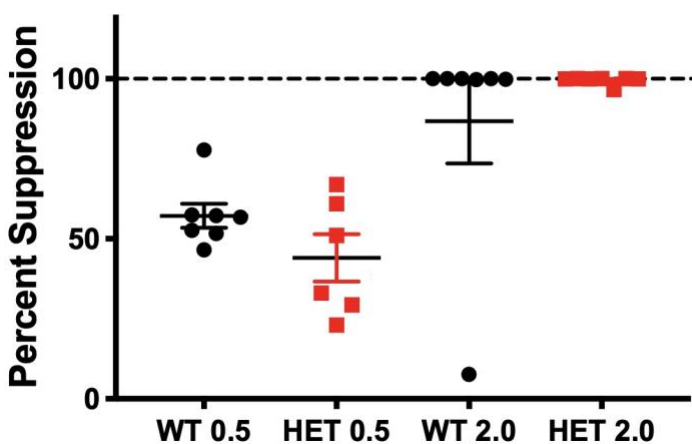
* patient mutation at the R209 position but change is not arginine(R) to histidine(H)

Supplemental Table 2. Gait analysis parameters of female *Gnao1* R209H mutant mice

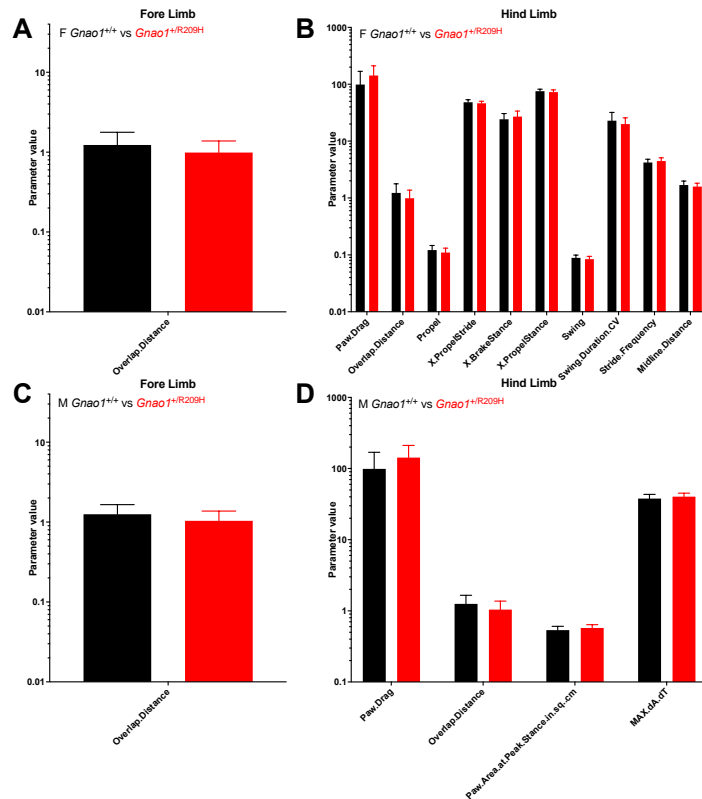
Measured Parameters	Fore Limb		Hind Limb		Fore Limb						Hind Limb					
	P value	FDR	P value	FDR	F WT Mean	SD	N	F R209H Mean	SD	N	F WT Mean	SD	N	F R209H Mean	SD	N
Swing	0.000862	No	0.001686	Yes	0.088759	0.011161	166	0.09418182	0.013945	88	0.0841024	0.0102	166	0.08846591	0.010834	88
X.SwingStride	0.553568	No	0.784138	No	38.269277	3.355496	166	38.53295455	3.399754	88	36.083735	4.11783	166	35.93068182	4.442386	88
Brake	0.257048	No	0.198976	No	0.0732651	0.016007	166	0.07582955	0.019054	88	0.0411506	0.013145	166	0.03895455	0.012517	88
X.BrakeStride	0.239615	No	0.003087	No	31.40241	4.642243	166	30.67613636	4.729754	88	17.425904	4.881231	166	15.58409091	4.255784	88
Propel	0.062971	No	0.000237	Yes	0.0713374	0.017694	166	0.07560227	0.016582	88	0.1098855	0.021791	166	0.12122727	0.025295	88
X.PropelStride	0.457782	No	0.000572	Yes	30.322289	4.635664	166	30.7875	4.943423	88	46.489157	3.90007	166	48.48409091	5.061345	88
Stance	0.052934	No	0.019444	No	0.1446145	0.026021	166	0.15142045	0.027503	88	0.1510843	0.028399	166	0.16014773	0.030727	88
X.StanceStride	0.553568	No	0.784138	No	61.730723	3.355496	166	61.46704545	3.399754	88	63.916265	4.11783	166	64.06931818	4.442386	88
Stride	0.009436	No	0.003393	No	0.2334036	0.033972	166	0.24563636	0.038132	88	0.2352108	0.03372	166	0.24863636	0.035716	88
X.BrakeStance	0.314746	No	0.001422	Yes	50.877108	6.954237	166	49.93863636	7.271317	88	27.063855	6.667062	166	24.28409091	6.276995	88
X.PropelStance	0.314746	No	0.001422	Yes	49.122892	6.954237	166	50.06136364	7.271317	88	72.936145	6.667062	166	75.71590909	6.276995	88
Stance.Swing	0.554245	No	0.625985	No	1.6361446	0.235657	166	1.61818182	0.218955	88	1.8054217	0.324599	166	1.82727273	0.36632	88
Stride.Length	0.920542	No	0.777101	No	5.836747	0.776261	166	5.82613636	0.859229	88	5.8759036	0.758562	166	5.90568182	0.864811	88
Stride.Frequency	0.014077	No	0.002251	Yes	4.5030121	0.657122	166	4.28636364	0.678264	88	4.4710843	0.641689	166	4.21590909	0.598059	88
PawAngle	0.094114	No	0.886736	No	-1.226506	4.09998	166	-0.36022727	3.519944	88	0.7493976	15.44145	166	0.45227273	16.46886	88
Absolute.PawAngle	0.008759	No	0.141453	No	3.673494	2.178745	166	2.94204545	1.940655	88	14.766265	4.431629	166	15.65681818	4.845256	88
Paw.Angle.Variability	0.273075	No	0.075906	No	6.5048193	1.980413	166	6.20113636	2.301149	88	4.7891566	1.885737	166	5.24431818	2.029884	88
Stance.Width	0.48535	No	0.502257	No	3.5240964	2.863891	166	3.79545455	3.093037	88	7.560241	6.89068	166	8.19318182	7.600451	88
StepAngle	0.829913	No	0.607524	No	62.024096	67.35433	166	60.11363636	67.41746	88	34.722892	45.03798	166	37.97727273	53.14521	88
SLVar	0.178551	No	0.006484	No	1.0621687	0.280301	166	1.11465909	0.321265	88	0.8433133	0.275812	166	0.97397272	0.48285	88
SWVar	0.620186	No	0.655617	No	14.644578	15.3228	166	15.68181818	16.8117	88	6.560241	6.824598	166	6.97727273	7.549039	88
StepAngleVar	0.52429	No	0.895657	No	61.03012	78.19598	166	54.72727273	68.41115	88	52.662651	67.93058	166	53.84090909	68.31551	88
X.Steps	0.134323	No	0.121155	No	27.427711	6.803579	166	26.14772727	5.759629	88	27.274096	6.745719	166	25.94886364	5.887372	88
Stride.Length.CV	0.237484	No	0.006673	No	18.675843	0.063927	166	19.66806818	6.872459	88	14.471386	4.888988	166	16.61125	7.523195	88
Stance.Width.CV	0.865848	No	0.556665	No	50.23494	55.10375	166	51.48863636	58.28448	88	72.174699	94.41713	166	79.59090909	97.67394	88
Step.Angle.CV	0.162584	No	0.685476	No	51.463855	72.44272	166	65.53409091	82.82733	88	67.572289	81.02243	166	72	86.10726	88
Swing.Duration.CV	0.294853	No	0.002003	Yes	25.371325	7.757021	166	24.28715909	7.973726	88	20.003675	5.795205	166	22.93125	9.096783	88
Paw.Area.at.Peak.Stance.In.ag.cr	0.00641	No	0.66547	No	0.2454217	0.046964	166	0.2625	0.047398	88	0.5005422	0.079416	166	0.49590909	0.084386	88
Paw.Area.Variability.at.Peak.Stan	0.166619	No	0.005094	No	0.0223494	0.0077	166	0.02363636	0.009276	88	0.0453615	0.016391	166	0.05272727	0.024947	88
Hind.Limb.Shared.Stance.Time			0.537429	No	1	0	166	1	0	88	17.277108	21.25847	166	19.07954545	23.70665	88
X.Shared.Stance			0.630463	No	1	0	166	1	0	88	97.849398	53.24314	166	101.2954546	56.13001	88
StanceFactor	0.369433	No	0.629805	No	9.3192771	9.282136	166	8.26136364	8.197973	88	10.120482	9.739514	166	10.76136364	10.67169	88
Gait.Symmetry	0.140168	No	0.140168	No	1.0078313	0.026056	166	1.01545455	0.055974	88	1.0078313	0.026056	166	1.01545455	0.055974	88
MAX.dA.dT	0.013856	No	0.798156	No	12.997831	2.686344	166	13.86136364	2.557019	88	34.648434	6.534348	166	34.42875	6.45687	88
MIN.dA.dT	0.020047	No	0.170644	No	-3.557771	0.714287	166	-3.82125	1.069478	88	-7.6283133	1.321913	166	-7.84977273	1.00655	88
Tau.Propulsion			0.758007	No	1	0	166	1	0	88	112	61.46583	166	109.4545455	64.65877	88
Overlap.Distance	0.000061	Yes	0.000061	Yes	0.9884337	0.392521	166	1.23068182	0.543744	88	0.9884337	0.392521	166	1.23068182	0.543744	88
Paw.Placement.Positioning.PPP	0.110841	No	0.110841	No	0.4084337	0.147262	166	0.44352273	0.197449	88	0.4084337	0.147262	166	0.44352273	0.197449	88
Ataxia.Coefficient	0.291223	No	0.016224	No	0.7913855	0.292622	166	0.83193182	0.305505	88	0.6390964	0.254344	166	0.72945455	0.331666	88
Midline.Distance	0.495964	No	0.002418	Yes	-1.795783	0.305625	166	-1.82375	0.321102	88	1.5896988	0.233483	166	1.69352273	0.296365	88
Axis.Distance	0.755914	No	0.937074	No	0.003253	0.750176	166	-0.02784091	0.771926	88	-0.0086145	1.19335	166	-0.02136364	1.27859	88
Paw.Drag			0.000004	Yes	1	0	166	1	0	88	142.39157	69.54238	166	99.01136364	70.34978	88

Supplemental Table 3. Gait analysis parameters of male *Gnao1* R209H mutant mice

Measured Parameters	Fore Limb		Hind Limb		Fore Limb								Hind Limb							
	P value	FDR	P value	FDR	M WT Mean	SD	N	M R209H Mean	SD	N	M WT Mean	SD	N	M R209H Mean	SD	N				
Swing	0.742713	No	0.849568	No	0.09575	0.010045	112	0.09525	0.011893	96	0.08889286	0.009719	112	0.08860417	0.012193	96				
X.SwingStride	0.186611	No	0.414505	No	39.058929	3.751313	112	38.39479167	3.422753	96	36.2732143	4.576024	112	35.76979167	4.245595	96				
Brake	0.07883	No	0.352604	No	0.0748482	0.018216	112	0.07973958	0.021724	96	0.03811607	0.011977	112	0.03653125	0.012519	96				
X.BrakeStride	0.046618	No	0.281478	No	30.158036	5.195713	112	31.809375	6.68853	96	15.1651786	3.560158	112	14.56770833	4.416536	96				
Propel	0.476735	No	0.246967	No	0.0765714	0.02064	112	0.074625	0.018382	96	0.12082143	0.021481	112	0.12441667	0.023144	96				
X.PropelStride	0.224488	No	0.043317	No	30.778571	5.958209	112	29.796875	5.594329	96	48.5633929	3.628342	112	49.66354167	4.175722	96				
Stance	0.459252	No	0.617997	No	0.1515089	0.02807	112	0.15432292	0.026341	96	0.15891964	0.029695	112	0.1609375	0.028273	96				
X.StanceStride	0.186611	No	0.414505	No	60.941071	3.751313	112	61.60520833	3.422753	96	63.7267857	4.576024	112	64.23020833	4.245595	96				
Stride	0.606739	No	0.701773	No	0.2472232	0.03416	112	0.24967708	0.034296	96	0.24777679	0.033051	112	0.2495625	0.033977	96				
X.BrakeStance	0.144106	No	0.130071	No	49.605357	8.646812	112	51.459375	9.584303	96	23.6625	4.618239	112	22.54375	5.984204	96				
X.PropelStance	0.143904	No	0.129692	No	50.395536	8.64638	112	48.540625	9.584303	96	76.3375	4.618239	112	77.45729167	5.983552	96				
Stance.Swing	0.254797	No	0.507041	No	1.5875	0.262395	112	1.628125	0.247813	96	1.80178571	0.371018	112	1.83645833	0.379784	96				
Stride.Length	0.514326	No	0.397668	No	6.2089286	0.784024	112	6.1375	0.788636	96	6.23035714	0.794104	112	6.13854167	0.76066	96				
Stride.Frequency	0.599868	No	0.814209	No	4.2294643	0.586429	112	4.18645833	0.590917	96	4.21964286	0.559736	112	4.20104167	0.578291	96				
PawAngle	0.409773	No	0.901338	No	-1.589286	3.516355	112	-1.11875	4.682854	96	1.14821429	17.7401	112	0.85520833	16.02805	96				
Absolute.PawAngle	0.056783	No	0.005873	No	3.075	2.31787	112	3.77708333	2.962662	96	17.0785714	4.6622	112	15.265625	4.705849	96				
Paw.Angle.Variability	0.708628	No	0.031802	No	6.4607143	2.427261	112	6.57083333	1.67997	96	4.3625	1.635481	112	4.95104167	2.276886	96				
Stance.Width	0.384371	No	0.887767	No	3.4107143	2.559397	112	3.11458333	2.298145	96	7.05357143	6.172942	112	7.17708333	6.412151	96				
Step.Angle	0.543298	No	0.524421	No	48.8125	54.21986	112	53.5625	58.20288	96	31.9732143	43.08831	112	28.34375	38.24184	96				
SLVar	0.435215	No	0.15068	No	1.0917857	0.27152	112	1.13145833	0.449982	96	0.83419643	0.271292	112	0.89395833	0.326185	96				
SWVar	0.920715	No	0.253516	No	12.625	12.67695	112	12.44791667	12.89053	96	5.17857143	5.429672	112	6.15625	6.875323	96				
Step.Angle.Var	0.24211	No	0.876653	No	45.919643	60.59437	112	56.60416667	70.76982	96	46.75	60.6561	112	48.04166667	58.69079	96				
X.Steps	0.8498	No	0.63707	No	24.424107	4.986563	112	24.5625	5.537076	96	24.3080357	4.825909	112	24.65104167	5.644336	96				
Stride.Length.CV	0.286712	No	0.057982	No	17.998393	5.348469	112	19.09291667	9.18012	96	13.5108036	4.479219	112	14.95729167	6.409749	96				
Stance.Width.CV	0.642162	No	0.33056	No	31.107143	36.02711	112	33.63541667	42.3313	96	65.6696429	74.19895	112	76.25	82.21333	96				
Step.Angle.CV	0.453618	No	0.810819	No	49.205357	63.63878	112	42.73958333	59.83877	96	52.7767857	64.92819	112	54.9375	64.68544	96				
Swing.Duration.CV	0.065786	No	0.040295	No	24.166161	6.335163	112	26.689375	12.71546	96	19.8541964	5.777298	112	21.98125	8.948453	96				
Paw.Area.at.Peak.Stance.in.sq.cm	0.269777	No	0.000048	Yes	0.2744643	0.031902	112	0.2796875	0.036171	96	0.57464286	0.063401	112	0.53677083	0.068032	96				
Paw.Area.Variability.at.Paw.Stan	0.906173	No	0.815503	No	0.0205357	0.010209	112	0.02072917	0.013396	96	0.044375	0.019162	112	0.04375	0.019317	96				
Hind.Limb.Shared.Stance.Time			0.757282	No	1	0	112	1	0	96	16.2678571	19.84035	112	17.125	19.99961	96				
X.Shared.Stance			0.36289	No	1	0	112	1	0	96	82.4196429	46.81026	112	88.27083333	45.32908	96				
StanceFactor	0.904653	No	0.985628	No	9.5178571	9.432532	112	9.67708333	9.675248	96	10.7142857	10.60293	112	10.6875	10.76477	96				
Gait.Symmetry	0.339967	No	0.339967	No	1.0023214	0.026913	112	0.9975	0.044745	96	1.00232143	0.028913	112	0.9975	0.044745	96				
Max.dA.dT	0.337523	No	0.000739	Yes	14.877321	2.009157	112	15.17510417	2.457478	96	40.355625	4.795198	112	37.9240625	5.440301	96				
MIN.dA.dT	0.043386	No	0.215019	No	-3.363571	0.813505	112	-3.645625	1.177005	96	-7.7479464	1.135325	112	-7.51552083	1.551981	96				
Tau.Propulsion			0.069796	No	1	0	112	1	0	96	90.5625	46.16808	112	104.5729167	64.28223	96				
Overlap.Distance	0.00004	Yes	0.00004	Yes	1.0380357	0.333044	112	1.251875	0.401419	96	1.03803571	0.333044	112	1.251875	0.401419	96				
Paw.Placement.Positioning.PPP	0.072965	No	0.072965	No	0.4177679	0.151887	112	0.4609375	0.193277	96	0.41776786	0.151887	112	0.4609375	0.193277	96				
Ataxia.Coefficient	0.131163	No	0.062689	No	0.7350893	0.247932	112	0.805625	0.413488	96	0.58044643	0.24559	112	0.65375	0.31857	96				
Midline.Distance	0.193089	No	0.49868	No	-1.933214	0.331655	112	-1.9984375	0.388778	96	1.52928571	0.19725	112	1.506875	0.277653	96				
Axis.Distance	0.734326	No	0.867511	No	0.0076786	0.789782	112	-0.02947917	0.781835	96	0.01223214	1.234583	112	-0.01677083	1.264412	96				
Paw.Drag			0.141646	No	1	0	112	1	0	96	108.973214	56.80795	112	96.90625	61.0565	96				



Supplemental Figure 1. WT and *Gnao1*^{+/*R209H*} mice show no difference in percent suppression of locomotion after risperidone treatment *Gnao1*^{+/*R209H*} mice show similar sensitivity to risperidone treatment at 2.0 mg/kg or 0.5 mg/kg compared to WT treated mice, unpaired Student's *t*-test.



Supplemental Figure 2. False discovery rate (FDR) calculation probed of significantly different parameters from the DigiGait data in *Gnao1*^{+/R209H} mice. All parameters that showed significance are plotted here. (A&B) Female *Gnao1*^{+/R209H} and their littermate controls showed 9 parameters with significance detected by the FDR analysis. (C&D) Male *Gnao1*^{+/R209H} and their littermates controls exhibited fewer parameters with significance comparing to female detected by the FDR analysis in fore and hind limb data combined. FDR is calculated by a two-stage step-up method of Benjamini, Krieger and Yekutieli. Significant values are defined as $q < 0.01$.